

Long-Period Superlattice Pd₃Mn II and Its Large Tetragonal Distortion

HIROSHI SATO AND ROBERT S. TOTH

Scientific Laboratory, Ford Motor Company, Dearborn, Michigan

(Received 1 April 1965)

The origin of the stabilization of the long-period structure in a transition-metal alloy and of the large tetragonal distortion which is a function of the composition in such an alloy series has been investigated. For this purpose characteristics of the long-period superlattice Pd₃Mn II were investigated over a wide composition range in relation to its neighboring phases in the Pd-Mn system. It was found that a Cu₃Au-type superlattice exists at Mn compositions below 25 at.%, while for Mn contents above the Pd₃Mn II range, a CuAu-type superlattice is formed. The concentration range with the CuAu-type ordered structure had previously been reported as an independent β_1 phase with a tetragonally distorted CsCl-type structure. Moreover, as the Mn content increases, the cubic A_2B -type superlattice was found to transform continuously to the AB -type superlattice through the long-period structure without the formation of a two-phase region. Pd₃Mn II has a fixed domain size of $M=2$, irrespective of the composition in its range of stability. This structure was found to be stabilized by a tetragonal distortion which keeps the Brillouin-zone boundaries at the Fermi surface as the electron-atom ratio varies, instead of by changing the period of the structure as observed in other long-period superlattices. The large distortion which occurs above the stoichiometric composition is sustained by a preferential distribution of the excess Mn atoms. From these observations it was concluded that the origin of the stability in Pd₃Mn II is similar to that in the noble-metal alloys with long-period structures, and hence the number of conduction electrons of the Mn and Pd atoms could be deduced to be 3 and 0.6, respectively.

I. INTRODUCTION

THE formation of a superlattice has recently been reported around the 3:1 composition in the α -phase region of the Pd-Mn system after a prolonged annealing treatment.^{1,2} Previous investigations had indicated that this region is devoid of any solid-state transformations.^{3,4} A phase diagram of the Pd-Mn system previously constructed is shown in Fig. 1 for reference. This alloy, Pd₃Mn, was found to have an ordered fcc structure with periodic antiphase domains (or a one-dimensional long-period superlattice⁵). The unit cell of this superlattice, which was determined by electron diffraction on single-crystal films,¹ as well as by neutron diffraction of polycrystalline bulk samples,² is shown in Fig. 2. It can be seen that the alloy has a one-dimensional long-period structure of the Ag₃Mg type with a domain size M exactly equal to two.

The occurrence of this structure in the Pd-Mn system is of interest mainly for the following two reasons. In the first place, the alloy is composed of transition metals only, and not of noble metals, as in other alloys with a long-period structure.⁶ In the second place, the periodicity does not seem to change with a change in composition, or electron-atom ratio of the system, whereas in long-period superlattices of the noble metals, the periods ($2M$) do change continuously as a function of the electron-atom ratio. The domain size, or the half period M , of the structure as measured on single-crystal thin-film specimens¹ and on polycrystalline bulk samples² was found to be exactly equal to two, irre-

spective of the fact that the composition, especially those of the thin-film specimens, tended to be off the stoichiometric composition. Therefore, it appeared highly probable that the M value is insensitive to the composition and keeps the same value with a small change in composition.

A theory of the formation of long-period superlattices has been worked out based on the noble-metal alloys.⁵⁻⁸ According to the theory, the long-period superlattice gains its stability through the reduction

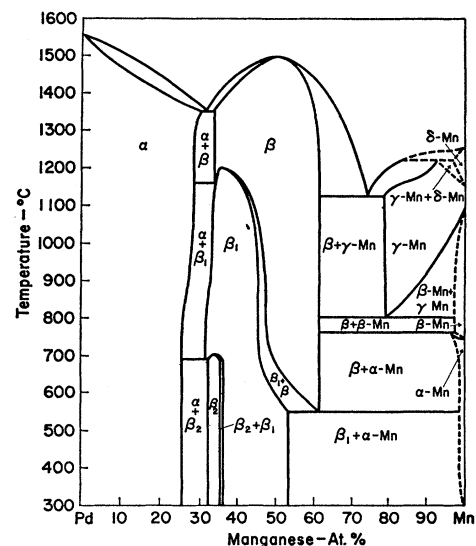


Fig. 1. Phase diagram of the Pd-Mn system by Raub and Mahler [M. Hansen and K. Anderko, *Constitution of Binary Alloys* (McGraw-Hill Book Company, Inc., New York, 1958), p. 944].

¹ H. Sato and R. S. Toth, Phys. Rev. Letters 8, 239 (1962).

² R. S. Toth and H. Sato, J. Appl. Phys. 33, 3250 (1962).

¹ D. Watanabe, Trans. Japan Inst. Metals 3, 234 (1962).

² J. W. Cable, E. O. Wollan, W. C. Koehler, and H. R. Child, Phys. Rev. 128, 2118 (1962).

³ G. Grube and O. Winkler, Z. Elektrochem. 42, 815 (1936).

⁴ E. Raub and W. Mahler, Z. Metallk. 45, 430 (1954).

⁵ H. Sato and R. S. Toth, Phys. Rev. 124, 1833 (1961).

⁶ H. Sato and R. S. Toth, Phys. Rev. 127, 469 (1962).

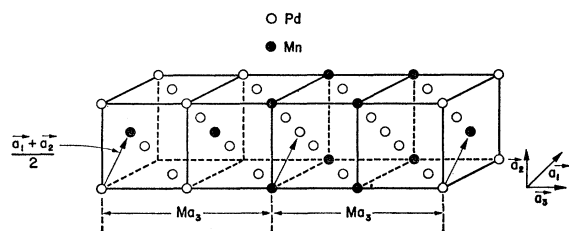


FIG. 2. Unit cell of the structure $\text{Pd}_3\text{Mn II}$. The unit cell is divided into two antiphase domains of size $M=2$

in the Fermi energy by bringing the Brillouin-zone boundaries into contact with the Fermi surface of the alloy. Thus, the superperiod of the alloy is determined by the size of the Fermi surface, or equivalently, by the electron-atom ratio of the system. In the case of noble-metal alloys, the number of valence electrons of the constituent atoms is known, and the period can be predicted from the electron-atom ratio of the system by the above theory. The problem involved here is whether this theory can also be applied, in principle, to transition-metal alloys having a superperiod. If this is found to be the case, it would then be possible to deduce the number of conduction electrons of each constituent transition element. This knowledge has been repeatedly sought after but usually with controversial results.

The antiphase boundaries, which must be present in a superperiodic system, introduce a surface-energy term which is referred to as the antiphase boundary energy. This energy term competes with the reduction in the electron energy mentioned above in determining whether a long-period structure will be formed, and if one is formed, the period of the structure is determined by the resultant minimum of these two energy terms. As long as the period of the system is large, the antiphase boundaries can be treated as a simple perturbation and the antiphase boundary energy can be treated independently of the electron energy. When the period becomes shorter, however, the antiphase boundary energy cannot be treated independently, and this energy per boundary, if we still try to keep this expression, is expected to increase in a complicated way. Experimentally, the half-period $M=2$ is considered to be about the limit of the simple treatment outlined above. The observed M value in usual long-period superlattices is nonintegral and this is interpreted as a mixture of domains with different M values. In order to have a resultant period less than two, it is necessary to introduce domains with $M=1$ in the system, where the antiphase boundary exists at every fcc unit-cell period, and hence the antiphase domain boundary energy is thought to be very high. Whether the $M=2$ case is the actual limit, or whether a mixture of $M=2$ and $M=1$ can exist, depends on the magnitude of the antiphase domain boundary energy, and hence on the type of alloy. For example, in the CuAu II alloys containing additional elements⁵ or in the Ag-Mg alloys

around Ag_3Mg ,^{6,9,10} the period can be made shorter than two, by changing the electron-atom ratio of the system, although there is a tendency in these alloys to stick to the $M=2$ value.⁶ On the other hand, in the Au-Zn $\text{Au}_3\text{Zn(H)}$ and Au-Cd (Au_3Cd) alloys, over the small ranges of composition in which these alloys are stable, the period seems to be fixed at $M=2$.^{6,11,12}

In view of the mechanism of stabilization of the long-period superlattice, it would be instructive to know what would be the consequence of changing the e/a ratio of a system having an $M=2$ structure, provided that the alloy retains the same antiphase structure. In the case of $\text{Au}_3\text{Zn(H)}$, Au_3Cd , etc., the existing region of the long-period structure is so narrow that it is impossible to draw any reasonable conclusions on this question. However, the Pd-Mn alloys around Pd_3Mn seem to retain the $M=2$ structure over a reasonable composition range, and hence can be considered to be an interesting example for the investigation of this effect.

Since the problem involved here is in determining the change in crystallographic structure for alloys over a wide composition range, an exact knowledge of the phase diagram is required. As the previously published phase diagrams are at least incomplete, we have undertaken to shed further light on the phase region around Pd_3Mn .

In the paragraphs below, we will present data on the structure of Pd-Mn alloys with Mn contents from about 10 to 45 at. % as obtained from measurements on single-crystal thin films and bulk powdered material. The data will show that a hitherto undetected Cu_3Au -type ordered structure exists at Mn contents below the range of the long-period structure, while above that range a CuAu I -type structure is formed. A rather unusual characteristic of these alloys will be described whereby the Cu_3Au -type superlattice transforms continuously to the CuAu I -type while passing through the tetragonally distorted periodic antiphase structure. This feature will be brought out through consideration of the symmetry and intensities of the diffraction patterns of these alloys. In the discussion of results, we will explain in detail, using the data combined with the general theory of the long-period superlattice, the characteristic features of these alloys in the following sequence: (a) We identify the structure of the β_1 phase as the CuAu I -type superstructure rather than a tetragonally distorted CsCl structure. (b) We establish the origin of stabilization of the long-period superlattice with fixed period in transition-metal alloys. (c) We determine the number of conduction electrons of Pd and Mn atoms in these alloys. (d) We account for

⁹ K. Schubert, B. Kiefer, M. Wilkens, and R. Hauffler, *Z. Metallk.* **46**, 692 (1955).

¹⁰ K. Fujiwara, M. Hirabayashi, D. Watanabe, and S. Ogawa, *J. Phys. Soc. Japan* **13**, 167 (1958).

¹¹ M. Hirabayashi and S. Ogawa, *Acta Met.* **9**, 264 (1961).

¹² H. Iwasaki, M. Hirabayashi, K. Fujiwara, D. Watanabe, and S. Ogawa, *J. Phys. Soc. Japan* **15**, 1771 (1960).

the tetragonal distortion in this structure and give the manner in which they may arise; and finally, we discuss the mode of transformation from the Cu₃Au to the CuAu-type ordered structure for this system.

II. EXPERIMENTAL RESULTS

The basic experimental technique used in this research to determine the crystal structures is the single-crystal thin-film method, whereby single-crystal films of the alloys in various orientations are produced by evaporation and their structure is examined mainly by transmission electron diffraction.

Single-crystal films of Pd-Mn alloys were obtained by first preparing single-crystal films of Pd and then diffusing in appropriate amounts of Mn to obtain alloys of desired composition. The films of Pd, with thicknesses of about 350–450 Å, were made by completely evaporating a weighed amount of high-purity Pd wire (99.9%) from a tungsten boat onto a heated single-crystal NaCl substrate. The freshly cleaved NaCl was first heated to about 500°C and the temperature was then reduced to between 310–340°C, which is the appropriate epitaxial temperature range for Pd in a conventional vacuum of 1×10^{-5} Torr. The Pd film was then floated off the substrate by immersion in water, and about 10–20 samples of the film were collected on standard 200-mesh stainless-steel microscope grids. These samples were then placed in a stainless-steel holder attached to a small furnace and mounted in exactly the same place where the rock-salt substrate was when the initial evaporation was made. Various amounts of high-purity Mn (99.99%) were evaporated onto the samples which were then annealed for several hours at temperatures about 400°C. The samples were then transferred to a small glass vacuum system where they were further annealed at temperatures of 600–700°C for about 20 h to allow ordering of the alloys. In some cases, various elements, such as Al, Cu, or Au were further added to the Pd-Mn alloys. This was done by repeating the procedure described above.

The structure of the alloys was then observed by transmission electron diffraction, using a 50-kV RCA-EDU unit. The lattice parameter of each alloy was determined by comparison with a Pt standard. Since there is always some uncertainty in the composition of thin-film alloys made by evaporation and since there was insufficient x-ray data on bulk material to which we could compare our lattice-parameter data to determine the composition, we also investigated the structure of eight bulk Pd-Mn alloys having compositions of 20, 23, 25, 28, 30, 34, 38, and 42 at.% Mn. Nine-gram boules of the alloys were made from high-purity Pd rod (99.99%) and electrolytic Mn (99.99%), which were melted in recrystallized alumina crucibles in a He atmosphere by high-frequency induction. The alloys were kept in a molten state for about 15 min to assure good mixing, and were then annealed just below the melting point

for about 1½ to 5 h. The positive pressure of He in the system kept the loss of Mn to a minimum. Slices of 25-mil thickness were cut from the center of the boule from which resistivity samples were cut and filings were obtained. The remaining portions of the slice were analyzed chemically to determine the composition. The resistivity samples and filings were vacuum encapsulated in small Vycor tubes and were annealed at temperatures from 760° to 400°C for times ranging from 30–40 days. The x-ray data on these bulk samples were obtained using Cu K_{α} or Co K_{α} radiation. Data were collected for each sample using a goniometer on a G.E. XRD unit and a Philips Debye-Scherrer camera. The main results obtained for thin-film and bulk-filed specimens are given below.

A. Thin Film

Using the procedure described above, excellent single-crystal films of Pd-Mn alloys were obtained. Around the 25% Mn composition, the Pd₃Mn periodic antiphase structure with $M=2$ was obtained and a transmission electron-diffraction pattern of this structure is shown in Fig. 3. An analysis of this pattern has been given by Watanabe¹ and is also explained below. At concentrations of Mn below 25%, the antiphase structure disappears and only an ordered Cu₃Au-type structure is formed. An example of a typical pattern is shown in Fig. 4. Diffraction patterns of this type of ordered structure are observed from near 25% Mn down to about 8% Mn. In order to distinguish the

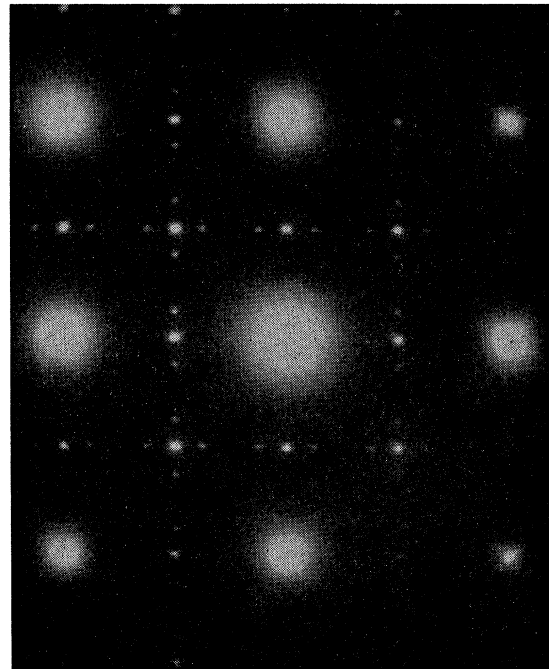


FIG. 3. Electron-diffraction pattern of an alloy having the Pd₃Mn II structure, showing the characteristic splitting of the superlattice spots.

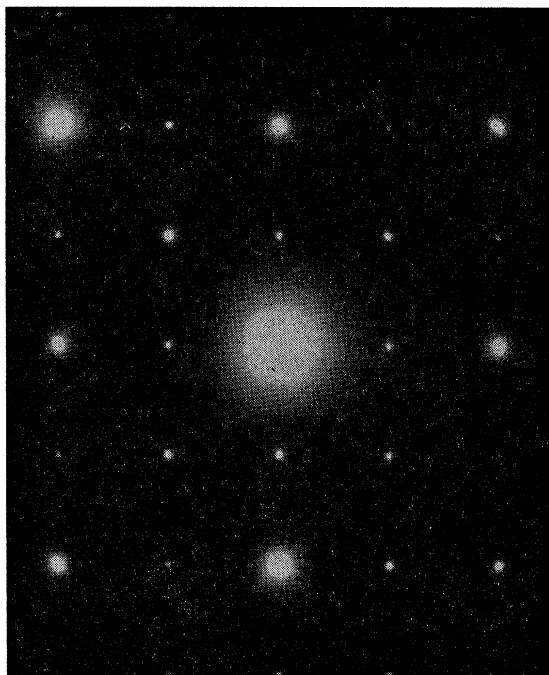


FIG. 4. Electron-diffraction pattern of a Pd-Mn alloy containing 20 at.% Mn which has the Cu_3Au -type ordered structure.

two types of ordered structures in this composition range, the long-period structure is referred to as Pd_3Mn II, as in the case of CuAu II, whereas the ordinary superlattice is referred to as Pd_3Mn I. The variation of lattice parameter versus composition is shown in Fig. 5 for the Pd_3Mn I alloys. A considerable spread in the data here may be attributed to the uncertainty in the composition of the alloys, which were determined by the known evaporated amounts of the material. There may also be some escape of Mn while annealing at high temperatures. Nevertheless it shows a general trend for an increase of the lattice parameter with the Mn content.

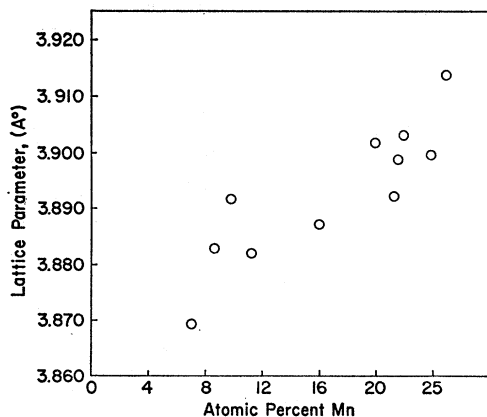


FIG. 5. Variation of lattice parameter with calculated composition for Pd-Mn alloys having the Cu_3Au -type ordered structure.

Above 25% Mn, the long-period structure with $M=2$ was stable, but it was found that the crystal begins to distort tetragonally with the c axis in the direction of the period of the structure. The distortion, with $c/a < 1$, increases continuously with the Mn content. An example of such a pattern is shown in Fig. 6, for an alloy where $c/a \sim 0.95$. This pattern with asymmetrically split superlattice spots can be interpreted, as in the cubic case, in the following way with the help of Fig. 7: The antiphase boundary of this structure has an "out of step" of the first kind, where the step shift $\frac{1}{2}(\mathbf{a}_1 + \mathbf{a}_2)$ occurs normal to the direction of the period (\mathbf{a}_3) of the structure (Fig. 2). In such a case, only those superlattice reflections with mixed h and k will split in the $[00l]$ direction. Thus, only the $\{101\}$, $\{011\}$, $\{100\}$, and $\{010\}$ reflec-

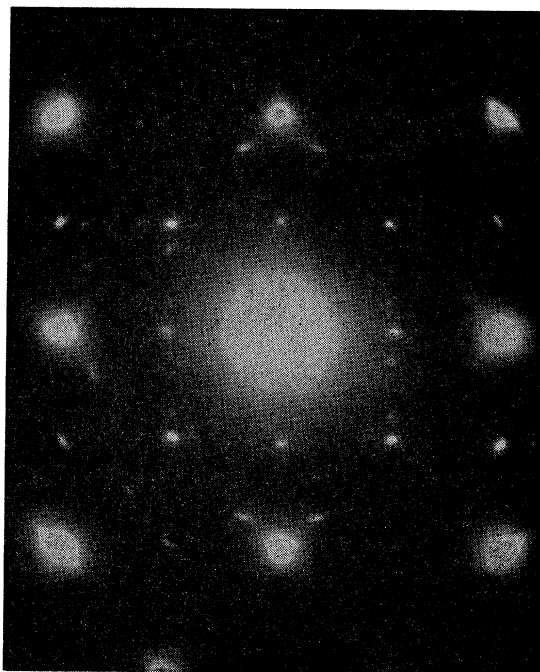


FIG. 6. Electron-diffraction pattern of an alloy having the Pd_3Mn II structure with a distortion $c/a \sim 0.95$.

tions will split, as shown in Fig. 7(a), (b), (c), while the $\{001\}$ and $\{110\}$ reflections remain unchanged. Since the diffraction pattern obtained is not from a single ordered domain, but is normally a composite obtained from mixtures of domains with the three possible orientations of the \mathbf{a}_3 axis in the film, the superposition of the three \mathbf{a}_3 orientations describes the pattern explicitly [Fig. 7(d)]. It is then clearly understood from the asymmetry of the split superlattice spots, that the tetragonal distortion is in the direction of the superperiod of the structure. In other words, the \mathbf{a}_3 axis is the c axis of the resulting tetragonal structure. The intensity of the superlattice spots should be equal if the distribution of domains in the three different orientations of the \mathbf{a}_3 axis is equal, with the intensity of the split

ones being approximately one-half that of the unsplit ones. An inequality in the distribution of these domains can thus be inferred from the relative intensities of these spots. The type of tetragonal distortion found here always occurs along with the formation of the long-period superlattice. However, the remarkable feature here is that the degree of distortion is far larger than those usually observed for long-period superlattices of noble-metal alloys, where the distortion is at most of the order of 1%.⁶

The long-period structure with fixed $M=2$ extends at least to about 32 at.% Mn with the tetragonality varying from $c/a=1$ at 25% Mn down to about 0.92 at about 32% Mn. This variation is shown in Fig. 8 for a systematic run on one series of alloy films. Again,

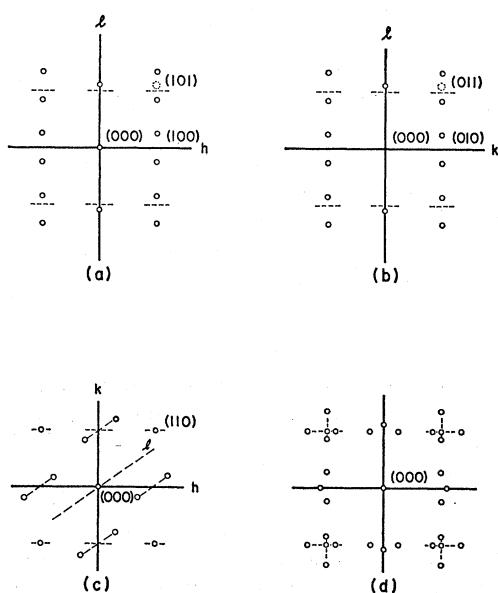


FIG. 7. Schematic intensity distribution of the inner set of superlattice spots in reciprocal space for three {100} planes through the origin for a Pd₃Mn II structure with tetragonal distortion in the c direction (a, b, c). The superposition of the three planes yields the pattern shown in (d). This type of superposition is usually observed experimentally as seen in Fig. 6.

the compositions were the calculated ones from known evaporated amounts and suffer the same uncertainties as mentioned above. Because of this uncertainty in the composition, the experimental points for the lattice parameters a and c for all the measured specimens were plotted against c/a and are shown in Fig. 9. The average atomic distance $(a^2c)^{1/3}$ is also plotted against c/a . Here c/a can be thought of as a measure of the composition. Unfortunately, $(a^2c)^{1/3}$ is extremely insensitive to the change of c/a and it is almost hopeless to utilize it as a measure of the composition even if the lattice constant of the alloy is known.

As the nominal Mn content increases, the intensities of the split superlattice spots decrease continuously while those of the unsplit spots remain strong and, at

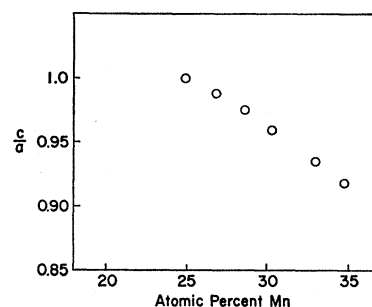


FIG. 8. Variation of the c/a ratio with calculated composition for an alloy series with the Pd₃Mn II structure.

around 34% Mn, only the unsplit spots remain. This is shown in Fig. 10. The symmetry of the superlattice spots in this figure corresponds to that of a CuAu I-type structure with equally distributed domains in three directions, and not that of the Cu₃Au-type alloys found at lower Mn content. If it were a Cu₃Au-type superlattice with a tetragonal distortion, the diffraction pattern should look like Fig. 11(a) or 11(b) depending on the distribution of the domains but not like Fig. 11(c), which represents the diffraction pattern shown in Fig. 10. The change in the relative intensity between the split and unsplit superlattice spots cannot be explained in terms of the inequality in the domain distribution and gives, therefore, the impression of a coexistence of two ordered phases. While changing from the Cu₃Au-type to the CuAu I-type, however, there seems to be no evidence for the coexistence of the Cu₃Au-type and CuAu I-type structure, such as might be seen in the superposition of patterns of two phases with distinctly different lattice constants. At still higher Mn contents the films became polycrystalline and no further investigations could be made. Up to this point the tetragonality continues to increase with the Mn content, with c/a decreasing continuously to 0.88.

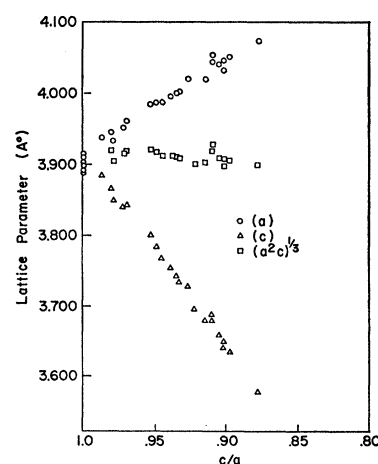


FIG. 9. Lattice parameters a and c versus c/a for ordered Pd-Mn alloys.

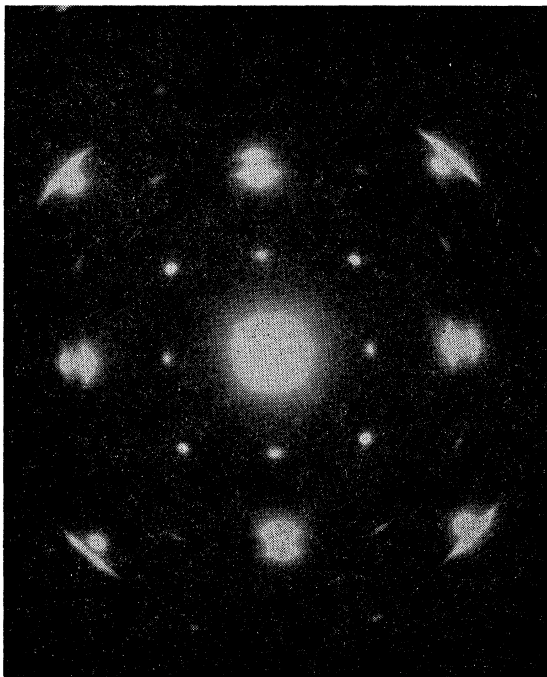


FIG. 10. Electron-diffraction pattern of a Pd-Mn alloy at around 34% Mn having the CuAu I structure.

In other words, the change in tetragonality and the diffraction pattern in general gives us the impression that these alloys remain as a homogeneous solid solution over the composition range described, although the

relative intensity of the superlattice spots varies in a way which indicates a two-phase coexistence.

As was done in the case of the long-period superlattice of the noble metals, the effect of additional elements on the c/a of the system and hence on the structure of the system was also investigated. The effect of Al was tested primarily, since Al is trivalent and the resultant change of the e/a ratio is expected to be large. Alloy films, having the Pd₃Mn structure with $c/a=1$, were first made and various amounts of Al were evaporated and diffused into the alloys. The net effect of the Al was to increase the tetragonality of the structure while still maintaining the $M=2$ period, a result similar to that obtained by simply increasing the Mn content. Although the exact quantity of added Al was very hard to determine, the increase in tetragonality followed closely that obtained by increasing the Mn content. The decrease in the intensity of the split superlattice spots as compared to the unsplit superlattice spots was again observed with the addition of Al. Thus, Al behaves approximately the same as additional Mn in these alloys. Although a sufficient number of samples (~ 10) were tested in order to ensure the reproducibility of the effect, the data are not shown here since we could not determine the composition with enough accuracy. The effect of the addition of Cu was also quite similar.

B. Bulk

In the case of bulk specimens the Pd-Mn filings with compositions 20, 23, 25, 28, 30, and 34% Mn were annealed from 770 to 525°C for a period of 34 days while the 38 and 42% alloys were annealed at 400°C for the same period of time. A chemical analysis of the composition of the alloys gave results consistent with the nominal ones above. However, since some systematic errors seem to be involved in the analysis, the nominal compositions are used here. The x-ray data on these alloys is summarized in Table I. Both the 20 and 23% Mn alloys showed evidence of the ordered Cu₃Au-type structure found in the thin films. The 25% alloy showed the splitting of the superlattice lines as did the 28% and 30% Mn alloys. The 28% Mn alloy showed some tendency toward tetragonality but was small, while the 30% alloy showed a $c/a=0.96$ which agrees very well with results obtained for the thin films. The inequality in the intensities of split and unsplit superlattice lines was also observed. Data for this alloy is shown in Table II along with that of the 34% Mn alloy. The 34% alloy has a face-centered tetragonal (fct) structure with a superlattice structure but with a c/a ratio greater than one. It thus corresponds to the β_2 phase found by Raub and Mahler,⁴ but the superlattice lines indicated there did not seem to agree exactly with what was found here. This structure, however, was not found in thin-film specimens. In Table II, only those lines with strong intensities are indexed based on the fct structure. The 38 and 42% alloys

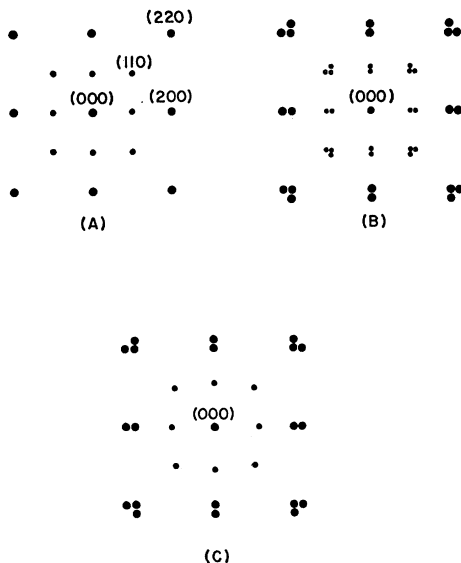


FIG. 11. Schematic intensity distribution of the inner set of superlattice spots and main spots in reciprocal space for a Cu₃Au-type superlattice with tetragonal distortion ($c/a < 1$), where (A) the c axis is normal to the plane of the film and (B) where domains distribute equally in three possible orientations. Part (C) is the pattern for a tetragonally distorted CuAu I-type superlattice where the domains distribute equally in three possible orientations.

show patterns which correspond to the β_1 structure determined by Raub and Mahler⁴ and confirmed by Yamauchi.¹³ These are described as CsCl-type ordered structures with a tetragonal distortion of $c/a \sim 1.25$ which varies with composition. However, we were not able to see the pattern corresponding to the μ phase as found by Yamauchi for a 40% Mn alloy with the present heat treatment. The resistivity-temperature curves were also measured for these alloys. However, the results do not seem to have any direct relation to the discussion given below and therefore the results are not given here.

III. DISCUSSION OF RESULTS

A. Summary of Experimental Data

Since the results of the experiments have some peculiar features, the major conclusions are first recapitulated to facilitate the discussions which follow.

In thin single-crystal films the basic structure of all the alloys up to about 40 at.% Mn can be interpreted as a face-centered tetragonal structure with c/a ranging from 1 to 0.88. The alloys in the range from 10 to 25% Mn are face-centered cubic with the Cu₃Au-type superlattice. Above 25% Mn, the structure becomes a regular one-dimensional long-period superlattice with $M=2$. However, when increasing the Mn content above 25% Mn, the lattice begins to distort tetragonally with the c axis in the direction of the superperiod. On further increasing the Mn content the intensity of the split superlattice spots decreases continuously, while that of the unsplit ones remains strong. This uniform decrease in intensity of the split spots cannot be explained by a change in the distribution of the ordered domains. Since the unsplit superlattice spots have the same symmetry as that of the tetragonal CuAu I-type structure with equal domain distribution, the structure of the alloys with high Mn content (up to 40% Mn), should be interpreted as having a tetragonal CuAu I-type ordered structure when the split spots disappear. The structure is clearly not that of the Cu₃Au-type structure having a tetragonal distortion. In other words, there is a continuous change of the ordered structures

TABLE I. Results of x-ray analysis on bulk powder samples of Pd-Mn alloys.

At.% Mn	Phase	Lattice constant	
		a (Å)	c/a
20	Pd ₃ Mn I	3.894	1
23	Pd ₃ Mn I	3.902	1
25	Pd ₃ Mn II	3.902	1
28	Pd ₃ Mn II	3.918	<1
30	Pd ₃ Mn II	3.956	0.96
34	β_2 (?)	3.844	1.05
38	β_1	2.872	1.26
42	β_1	2.884	1.25

TABLE II. X-ray data on three representative Pd-Mn alloys taken with Cu-K α radiation.

Line	2θ	Intensity	(hkl)	
30% Mn				
1	23.2	VVW	(10 1/4)	
2	23.3	W	(001)	
3	28.6	VW	(10 3/4)	
4	32.3	W	(110)	
5	37.2	VVW	(10 5/4)	
6	40.1	VS	(111)	
7	46.0	MS	(200)	
8	47.7	VVW	(10 7/4)	
9	47.9	M	(002)	
10	52.1	W	(021)	
11	59.3	VVW	(10 9/4)	
12	67.1	M	(220)	
13	68.3	MS	(202)	
14	80.9	MS	(131)	
15	83.6	M	(113)	
16	86.2	M	(222)	
17	116.6	M	(303)	
18	119.7	M	(313)	
34% Mn				
1	27.3	W		
2	29.6	W		
3	31.25	W		
4	35.4	W		
5	39.9	VS	(111)	
6	43.5	VW		
7	44.9	S	(002)	
8	47.3	S	(200)	
9	49.5	W		
10	56.3	VW		
11	58.2	VW		
12	61.6	VW		
13	65.5	W		
14	67.3	MS	(202)	
15	69.3	MS	(220)	
16	77.4	VW		
17	79.5	S	(113)	
18	83.0	MS	(131)	
19	86.4	MS	(222)	
20	90.3	VW		
38% Mn				
			as (CsCl)	as (CuAu)
			type	type
1	24.5	W	(001)	(001)
2	31.1	M	(100)	(110)
3	40.05	VS	(101)	(111)
4	44.6	S	(110)	(200)
5	50.5	M	(002)	(002)
6	51.6	W	(111)	(201)
7	60.7	W	(102)	(112)
8	64.9	M	(200)	(220)
9	69.6	MS	(112)	(202)
				(022)
10	74.0	W	(120)	(130)
11	79.0	MS	(003)	(003)
12	86.6	M	(202)	(311)
				(131)

from that of the Cu₃Au-type to the CuAu I-type through the long-period structure in the Cu₃Au-type ordered lattice. The c/a ratio in this composition range also changes continuously.

In the case of bulk, the results generally agree with that of the thin films in the low-Mn content range. However, at 34% Mn, although an ordered face-centered tetragonal structure is formed similar to that

¹³ H. Yamauchi, J. Phys. Soc. Japan **19**, 652 (1964).

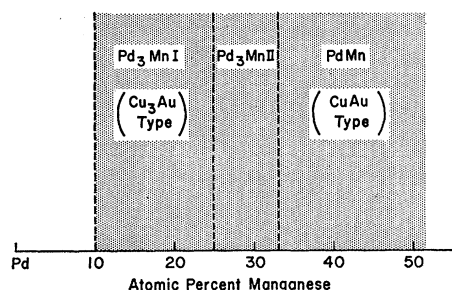


FIG. 12. Schematic phase distribution in the Pd-Mn system based on the presented data, showing the approximate stability range for the observed ordered structures.

in the thin-film specimens, the tetragonal distortion is just reverse (i.e., $c/a > 1$). Except for this particular alloy the alloys at higher Mn content gave a pattern which can be indexed as a tetragonally distorted CsCl-type superlattice with a $c/a \sim 1.25$, which decreases with increasing Mn content. This agrees with the previous investigations of the phase diagram of this system, and corresponds to the β_1 phase in the phase diagram. Existing ranges of these three types of superlattices in the Pd-Mn system based on our data are schematically shown in Fig. 12.

B. Structure of Alloys in the β -Phase Region

We would first like to point out the fact that the results on the bulk specimens in the β_1 -phase region do not contradict the thin-film results in the same composition range, which were interpreted in terms of a face-centered tetragonal lattice with c/a less than 1. A face-centered cubic structure can be thought of as a body-centered tetragonal structure with $c/a = \sqrt{2}$. The CuAu I-type superlattice with $c/a < 1$ corresponds, therefore, to a CsCl-type superlattice with a tetragonal distortion $c/a < \sqrt{2}$, which in most cases is still much larger than one. Since the films without the split superlattice spots have the CuAu I-type ordered structure and a distortion $c/a \sim 0.9$, the structure of these alloys corresponds exactly to the structure in the β_1 phase which has been described as a CsCl-type superlattice with a $c/a \sim 1.25$. However, from a physical point of view, the β_1 phase should be described as a CuAu I-type structure rather than a tetragonally distorted CsCl-type structure. The CuAu I-type superlattice has an atomic distribution with a tetragonal symmetry, and there is a natural tendency to have a tetragonal distortion with $c/a < 1$, which can be easily understood especially if a hard-ball model for atoms is assumed. On the other hand, the CsCl structure has an atomic distribution of cubic symmetry and it is hard to rationalize a tetragonal distortion in this structure without any particular reason. The c/a ratio of the β_1 phase decreases with Mn content and reaches a minimum at the stoichiometric 50-50 composition.^{4,14} This fact is a

¹⁴ K. Schubert, Z. Metallk. 46, 43 (1955).

natural consequence of a qualitative argument based on the simple geometrical model as above if one assumes a CuAu I-type structure. Furthermore, since the c/a ratio changes continuously from the α -solid-solution range into the β region as shown in the thin-film specimens, it would seem more natural to regard the β_1 phase as a continuation of the α phase, with a tetragonal distortion. A further support of this view will be given later (Sec. E). In the bulk specimens, however, one specimen with 34% Mn, shows a c/a ratio larger than one, and thereby separates the α - and β_1 -phase regions. This seems to correspond to the β_2 phase reported by Raub and Mahler⁴ (see Fig. 1). This structure, however, could not be observed in the single-crystal thin-film specimens. Since equilibrium can be reached much faster in thin-film samples than in bulk, and the elastic constraints, etc., for the transformation are much less, the true equilibrium phase should be more easily reached in the case of thin films. In view of these circumstances, the β_2 phase might not be a true equilibrium phase. Or, the difference might simply be due to the different impurity level of the two specimen forms. We did not investigate in detail the origin of this discrepancy.

C. Stabilization of the Long-Period Superlattice Pd₃Mn II

The next problem to consider is the stability of the long-period superlattice Pd₃Mn II. Here we would like to know whether the formation of the antiphase structure in transition-metal alloys, as in Pd-Mn has the same origin as in the noble-metal alloys already investigated. For this purpose a knowledge of the number of conduction electrons for both Pd and Mn is required so that the period of the system can be calculated from the established theory for noble-metal alloys. Unfortunately this information itself is quite controversial, and it should be deduced from other independent sources.

The neutron-diffraction measurements² of a 25% Mn alloy have shown that, when in the antiferromagnetic state, the Mn atom carries a magnetic moment of $4\mu_B$. Without the knowledge of the exact form factor, this implies that the number of d electrons of each Mn atom is either four or six. The number of conduction electrons is then either three or one, respectively. If the origin of the long-period superlattice in this alloy system is the same as in the noble-metal alloys, the number of conduction electrons which should be allocated to each atom can then be deduced from the equation which relates the electron-atom ratio of the alloys to the period of the long-period superlattice,⁶

$$e/a = (\pi/12\beta^3)(2 \pm 1/M + 1/4M^2)^{3/2} \quad (1)$$

using a reasonable value of the parameter t , which is a parameter arising from the nonsphericity of the Fermi surface, and putting $M = 2$. Depending on the signs in

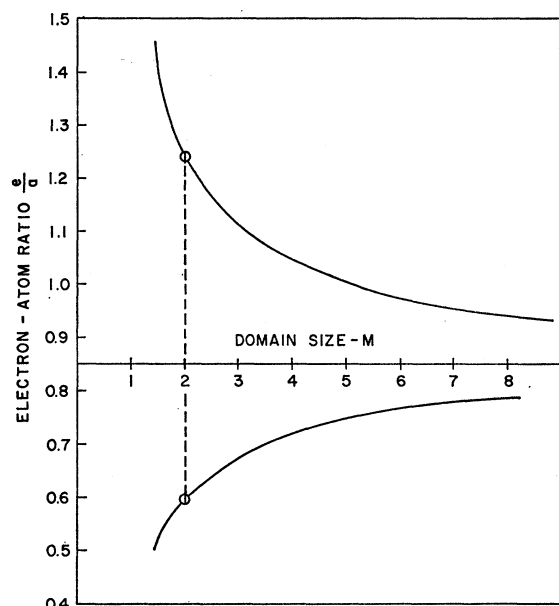


FIG. 13. Theoretical curves of electron-atom ratio versus domain size M based on Eq. 1 with $t=0.95$.

the equation, two values of e/a for the Pd atom can be calculated from the knowledge of each e/a for the Mn atom, from which a proper selection should be made. The theoretical curves based on Eq. (1) are shown in Fig. 13. One obtains, as two appropriate alternatives, an e/a value of 1 for Mn and 0.5 for Pd, using the negative sign in the equation (lower curve in Fig. 13), and with the positive sign (the upper branch), 3 for Mn and 0.6 for Pd, in each case assuming $t=0.95$, a value taken from results on the noble-metal alloys.⁶ Both combinations give quite reasonable values for the number of conduction electrons for the Pd atom. In order to determine the correct combination, additional information is required.

The relative stability of the long-period superlattice also depends on the size of the Fermi surface.^{8,15} The general conclusion is that a long-period superlattice tends to transform to an ordinary superlattice when the size of the Fermi surface, or the e/a ratio of the system, is changed in a direction which will make the period longer. Inversely one can also create a long-period superlattice from an ordinary superlattice in appropriate systems by changing the e/a ratio of the system in a direction which will make the period shorter according to Eq. (1). In the present Pd-Mn case, the e/a ratio of Pd is smaller than that of the Mn atom in both combinations, and therefore an increase in the Pd content will cause different effects depending on whether the alloys follow the upper curve [positive sign in Eq. (1)] or the lower curve [negative sign in Eq. (1)].

¹⁵ H. Sato and R. S. Toth, in *Alloying Behavior in Concentrated Solid Solutions*, edited by T. B. Massalski (Gordon and Breach Science Publishers, Inc., New York, to be published).

For the e/a combination, Mn=3 and Pd=0.6, an addition of Pd changes the e/a ratio of the system in the direction to decrease the stability of the structure, whereas, with the other combination, the system changes in a direction to increase the relative stability. The fact that the ordinary superlattice, Pd₃Mn I of the Cu₃Au-type appears at higher Pd contents implies that the system follows the upper curve of Eq. (1) and that 0.6 is therefore the probable number of conduction electrons for Pd in this system. This is also the value which is usually adopted for Pd in the solid state. The addition of Al affects the distortion of Pd₃Mn II in a similar way to the addition of Mn. In other words, Al atoms behave approximately the same as Mn atoms in the alloys. Since Al is trivalent, this also justifies the assumption of trivalency for the Mn atoms. Therefore, it seems reasonable to assume that the origin of the stability of Pd₃Mn II is the same as that of the long-period superlattices of the noble metals and the number of conduction electrons for Mn and Pd atoms is 3 and 0.6, respectively. This does not necessarily mean that the number of conduction electrons which each atom species contributes should be kept constant with a change in the composition. It would, therefore, be interesting to check by a measurement of the magnetic moment of Mn by neutron diffraction, for example, to see if the relative numbers of s and d electrons of these transition elements are kept unchanged for a considerable amount of change in alloying composition.

D. Distortion in Pd₃Mn II

In the common long-period superlattices in noble-metal alloys, nonintegral values of M are usually found.¹⁵ This has been interpreted as an average size resulting from a mixture of domains with different M values.⁵ Since such a mixture implies a lack of periodicity in the lattice, the electron energy is expected to be higher than in the case of integral values of M . Therefore, although the stability of the long-period structure with respect to the ordinary ordered structure due to the reduction in electron energy generally increases with decreasing period proportional to $1/M^2$,¹⁵ a periodic deviation in the energy from this curve would occur, with minima at each integral M value. As the M value decreases the relative change in period, and therefore the fluctuation in energy, becomes larger and as a result there would be a tendency for the alloy to remain at an integral M value. On the other hand, the antiphase domain boundary energy increases roughly as $1/M$ as the period becomes shorter, but is expected to increase sharply below $M=2$ from the reason discussed earlier. Because of these two conditions, there will be a sharp minimum in energy at $M=2$ and there is a strong tendency for alloys with a $M=2$ structure to remain at this value irrespective of a small variation in the e/a ratio of the system. Pd₃Mn II is considered to be such an example. Other examples are Au₃Zn(H),

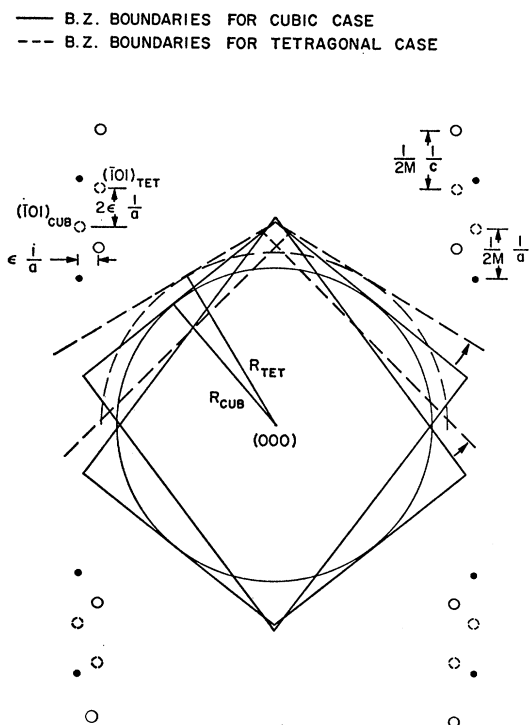


FIG. 14. Schematic drawing of the cross section of the Brillouin zone (B.Z.), which is originally formed by $\{110\}$ planes, in a plane through the origin and parallel to the (010) plane, showing the accommodation of a larger Fermi sphere by a tetragonal distortion in the direction of the superperiod.

Au_3Cd , etc. On the other hand, CuAu II with additional elements, Ag_3Mg , etc., are known to have values of M smaller than two. Even in these alloys, however, one can observe the tendency for the alloy to remain at the $M=2$ value.⁶ If alloys with an $M=1$ structure exist, as seems to be the case, this type of characteristic would be more pronounced. These alloys should then behave as intermetallic compounds. A study of the $M=1$ structure is currently underway.

Since the long-period superlattice is stabilized by bringing the Brillouin-zone boundaries into contact with the Fermi surface, this relation between the Brillouin-zone boundaries and the Fermi surface should be maintained as long as the alloy remains in the same structure. Therefore, if the e/a ratio is increased in a system with fixed period $M=2$, and the change in the period, as in the usual long-period structures, is not allowed, the way to accommodate the larger Fermi surface at the Brillouin-zone boundaries is by a tetragonal distortion ($c/a < 1$) of the crystal if the alloy remains in the same basic structure. This is shown schematically in Fig. 14. Then the distortion of the crystal with respect to the e/a ratio of the system can be calculated by introducing the tetragonal distortion parameter ϵ into Eq. (1), with $M=2$, where ϵ is defined as shown in Fig. 14. The resultant equation for alloys following the upper branch of the theoretical curve (with

a positive sign) is then given by

$$e/a = (\pi/12t^3)(2.5625 + 4.25\epsilon + 21.75\epsilon^2)^{3/2}, \quad (2)$$

where

$$c/a = 1 - 3\epsilon. \quad (3)$$

The tetragonality is in the direction of the period. If the e/a ratio is larger than the theoretical value for the $M=2$ structure, the distortion ϵ is positive and c/a is less than one. This corresponds to the case of $\text{Pd}_3\text{Mn II}$. The remarkable feature here is that this distortion is much larger and exactly opposite to that found for noble-metal alloys which follow the upper branch of the theoretical curve. In those alloys, the distortion was treated as a correction term arising from the mutual interaction between the Fermi surface and the Brillouin-zone boundaries. There, the lattice is distorted slightly (less than 1%) in order to make the period of the structure shorter for a fixed e/a ratio, thereby decreasing the electron energy of the structure. No exceptions to this rule have been found for the noble-metal alloys.^{6,15} In $\text{Pd}_3\text{Mn II}$, however, the distortion is not a secondary effect as in noble-metal alloys but a primary effect, because the period cannot be changed. The fact that the distortion is opposite in sign and large and that the distortion increases with the increase of the e/a ratio, suggests that the above mechanism is operative.

When the thin-film investigations were first made, the tetragonality in the Pd-Mn alloys was found to increase to 0.88 with the Mn content without a change in the basic structure, as described before. Since only polycrystalline films were obtained beyond the composition having $c/a=0.88$, it was thought this was the α -phase boundary. Based partly on the phase diagram of Raub and Mahler⁴ and taking into account the possible evaporation of Mn during annealing treatments, it was at first estimated that this boundary of the α -phase region was around 31 to 32 at.% Mn. Assuming that

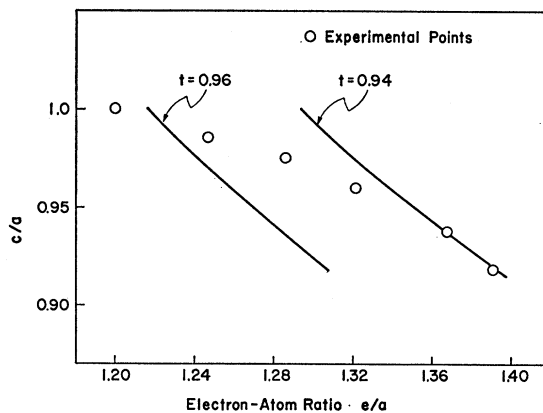


FIG. 15. Comparison of the experimental data and the theoretical curve based on Eq. (2) for the variation between the tetragonal distortion c/a and the electron-atom ratio e/a for two values of t .

the c/a ratio is a single-value function of the composition and that c/a takes the value 0.88 at 31~32 at.% Mn in Fig. 9, Eq. (2) with $t=0.96$ ¹⁶ gave good agreement with the experimental results, and was thought to be a quantitative proof of the above idea.¹⁷ However, since it was later found that the films with a larger c/a distortion seem to be in the composition range of the β phase, we cannot claim now that such an exact agreement exists. In Fig. 15 the calculated curve from Eq. (2), and the tetragonality of alloys which are definitely in the α -phase using the nominal Mn content are compared for both $t=0.96$ and 0.94. The agreement is still relatively good, and the discrepancy from the theoretical value is thought to represent a compromise between the electron and distortion energies in order to make the sum of these two terms a minimum. It may also be possible that the number of conduction electrons each atom contributes changes somewhat at higher composition in order to make the required distortion smaller. Why such a large distortion can be sustained by the alloy instead of changing its basic structure will be discussed below.

E. Phase Transformation: Pd₃Mn I \rightleftharpoons Pd₃Mn II \rightleftharpoons β -Phase

The manner in which the Pd₃Mn I superlattice changes into the CuAu-type superlattice in the β -phase region while passing through the Pd₃Mn II structure is peculiar to this system. As is shown in Fig. 4, the structure of Pd₃Mn I below 25 at.% Mn is cubic with the Cu₃Au-type superlattice. It should be pointed out, however, that the symmetry of the diffraction pattern of an A_3B -type (Cu₃Au-type) superlattice and an AB -type (CuAu I-type) superlattice is exactly the same if both are cubic and the three kinds of domains with different directions of the c axis for the AB superlattice mix equally. However, the intensity distribution of the diffraction pattern of Pd₃Mn II near 25% Mn can only be explained as being a one-dimensional long-period superlattice in an A_3B -type superlattice, with an equal mixing of the three possible domains, as was shown by Watanabe,¹ and not as an AB -type superlattice. Therefore the structure of the alloys at lower Mn contents (Pd₃Mn I) should definitely be of the A_3B -type superlattice and not the AB -type.

As the Mn content is increased above 25%, the long-period structure distorts with increasing tetragonality. The intensity distribution of the superlattice spots of such a distorted structure can again be explained as belonging to a long-period structure in an A_3B -type superlattice with the c axis in the direction of the super-period as shown in Fig. 7 and confirms the view that Pd₃Mn I is a superstructure of the Cu₃Au type. However, as the Mn content is further increased and as the degree of distortion further increases, the relative

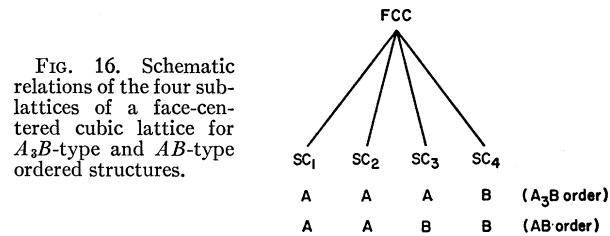


FIG. 16. Schematic relations of the four sublattices of a face-centered cubic lattice for A_3B -type and AB -type ordered structures.

intensities of the split and unsplit superlattice spots change as described above. This change in the relative intensities cannot be explained by a change in the distribution of domains of the long-period superlattice as can easily be understood by referring to the schematic figures in Fig. 7. Since the symmetry of the unsplit spots corresponds to that of a CuAu-type superlattice as shown in Fig. 11, the pattern at high Mn content gives the impression that it results from a superposition of the A_3B -type one-dimensional long-period superlattice and an AB -type superlattice, both however having the same lattice constant and c/a ratio. Or, we are led to conclude that the A_3B -type superlattice continuously changes into the AB -type superlattice through the long-period superlattice with the A_3B -type symmetry.

The difficulty in the former conclusion is obvious. The difficulty in the latter conclusion can also easily be seen from symmetry arguments. The face-centered cubic lattice can be divided into four interpenetrating simple-cubic sublattices SC₁, SC₂, SC₃, and SC₄ which are nearest neighbors. In the A_3B superlattice, three of them are occupied by A atoms and one is occupied by B atoms. On the other hand, in the AB superlattice, two are occupied by A atoms and the remaining two are occupied by B atoms (Fig. 16). When B atoms are added to the A_3B -type superlattice beyond the stoichiometric composition (25%), the excess B atoms should go equally into the A sublattices (SC₁, SC₂, and SC₃) as long as the A_3B symmetry is retained, whereas in the AB symmetry, the two A sublattices (SC₁ and SC₂) are occupied by A atoms exclusively but the two B sublattices (SC₃ and SC₄) are occupied equally by the remaining A and B atoms in a random fashion in this composition range. Usually, a definite phase boundary is observed between the A_3B -type and the AB -type superlattices as in the Cu-Au alloys (Cu₃Au and CuAu). Theoretically, if only the nearest-neighbor interaction is taken into account, only those alloys with the A_3B - (and AB_3 -) and the AB -type symmetries can exist and there should be a definite phase boundary between them¹⁸ and this can also be easily understood from a simple entropy argument. But if one of the three A sublattices of the A_3B -type superlattice, say SC₃, is preferentially occupied by excess B atoms, the A_3B -type superlattice can change into the AB -type superlattice continuously. However, in such a case, a lowering of the

¹⁶ In Ref. 17, the value of t was erroneously given to be 0.94. The actual value used was $t=0.96$.

¹⁷ H. Sato and R. S. Toth, Solid State Commun. 2, 249 (1964).

¹⁸ W. Shockley, J. Chem. Phys. 6, 130 (1938).

symmetry of the atomic distribution to an orthorhombic one occurs in the intermediate concentration range, and is neither cubic nor tetragonal as is observed in the Pd-Mn alloys. If a lattice distortion is not involved, the diffraction pattern cannot be distinguished from that of a homogeneous mixture of the A_3B - and the AB -type superlattices and it may not be necessary to rationalize the continuous transition. But this is not the case for the Pd-Mn alloys where there is a lattice distortion. Experimentally, such a continuous change of the A_3B -type superlattice into the AB -type superlattice has never been reported before.

If the A_3B -type superlattice has an antiphase structure like Pd₃Mn II, however, the difficulty mentioned above can be removed even with an actual distortion of the lattice. A one-dimensional long-period superlattice in an A_3B -type superlattice has a tetragonal symmetry and is tetragonally distorted in the direction of the superperiod. Because of this tetragonal distortion, the four sublattices are no longer equivalent and can be separated into two subgroups (SC₁ and SC₂, SC₃ and SC₄). Therefore, the excess B atoms can be occupied preferentially in the SC₃ sublattice. If the antiphase relation between two antiphase domains is of the first kind, SC₃ and SC₄ are alternately occupied by B atoms in each antiphase domain in the A_3B -type long-period superlattice. Therefore, the preferential distribution of the excess B atoms occurs equally in both the SC₃ and SC₄ sublattices, and the SC₃ and SC₄ sublattices become equivalent as a whole. This is then equivalent to the AB -type symmetry macroscopically with the c axis in the direction of the c axis of the A_3B -type long-period structure. In other words, the A_3B -type superlattice can change into the AB -type superlattice continuously by such a preferential occupation of the excess B atoms, without lowering the symmetry in the atomic distribution on a macroscopic scale. The intensity of the split superlattice spot is proportional to the difference in the scattering power of the A and B sublattices in the antiphase relation (SC₃ and SC₄). As the number of B atoms increases from the stoichiometric composition, B atoms enter preferentially into this A site in the manner explained above and the difference in the scattering power decreases monotonically, whereas the intensity of the unsplit superlattice spots depends on the difference in the scattering power of these two groups of sublattices. Therefore, the intensity of the unsplit spots increases with the B concentration but less steeply than the decrease in intensity of the split spots. This explains the observation of the change in the relative intensities of the superlattice spots.

The preferential distribution of Mn atoms in one of the A sublattices (SC₃ or SC₄, depending on the particular antiphase domain) in the antiphase structure introduces a tetragonal distortion because of the "size effect," which in turn compensates for the elastic energy required to distort the crystal in order to keep the

Brillouin zone at the Fermi surface, as discussed in the previous paragraph. This is the main reason why the Pd-Mn alloys tend to distort to such a large amount by the addition of Mn atoms to Pd₃Mn II, and why Pd₃Mn II can exist for a wide composition range with the same crystallographic form, keeping the Brillouin-zone boundaries at the Fermi surface and thereby reducing the electron energy. The actual tetragonal distortion is determined, therefore, mainly by the "size effect," deviating somewhat from the ideal distortion given by Eq. (2). The fact that all the constituent atoms are transition elements would also make such a large distortion easier compared to the case of noble-metal alloys where the filled d shell prohibits the approach of atoms beyond some limit. As the Mn content increases, the distinction between the two antiphase domains diminishes continuously and the reduction in the Fermi energy also decreases even if the Brillouin zone is kept at the Fermi surface. Therefore, at some concentration before it reached the stoichiometric composition (AB), the difference in electron energy necessary to make the SC₃ and SC₄ sublattices distinct (to form the long-period superlattice) becomes small enough and the SC₃ and SC₄ sublattices become equivalent as expected from the statistical thermodynamical treatment. This change may be detected by a minor change in the physical constants such as a discontinuous change in the c/a ratio or the lattice constant, etc., but without an appreciable change in the diffraction pattern. This change, however, could not be detected in the present case. Aside from these minor points, the Pd-Mn system is the first example where a continuous change from the A_3B -type structure to the AB -type is observed. The foregoing arguments also support the view that the β_1 phase is the continuation of the α phase and should not be treated as an independent body-centered tetragonal (bct) phase.

The preferential atomic distribution required to compensate for the elastic energy, which accompanies the distortion of the lattice, can occur in the usual type of long-period superlattice. This can occur not only in the manner described above, but also it may occur at the antiphase boundary. A segregation of this kind at the antiphase boundary can be a part of the actual lattice modulation which is mainly observed in the form of an asymmetry in intensity for pairs of split superlattice spots or as satellites flanking the normal spots in the diffraction pattern.¹⁹⁻²¹

IV. SUMMARY

Peculiar characteristics of a long-period superlattice in the transition-metal alloys, Pd₃Mn II were investigated in detail over a wide composition range in rela-

¹⁹ P. Perio and M. Tournari, *Acta Cryst.* **12**, 1044 (1959).

²⁰ G. Jehanno and P. Perio, *J. Phys. Radium* **23**, 854 (1962).

²¹ S. Fujime, D. Watanabe, S. Ogawa, K. Fujiwara, and S. Miyake, *J. Phys. Soc. Japan* **19**, 1881 (1964).

tion to the structures of other phases of the alloy system. In the composition range with lower Mn concentration, it was found that a Cu₃Au-type ordered structure, which had previously been undetected, exists in the α -phase region from 25 down to about 10 at.% Mn. On the other hand, at the higher Mn composition side of Pd₃Mn II, a CuAu I-type ordered structure exists with a c/a value which decreases as the equiatomic composition is reached. This phase was previously described as an independent β_1 phase having a tetragonally distorted CsCl-type superlattice. Several arguments are given which indicate that the β_1 phase is essentially a simple continuation of the α phase with basically the same face-centered cubic structure.

Pd₃Mn II is a one-dimensional long-period structure with a fixed domain size $M=2$. It exists over a considerably wide composition range (25 to about 32 at.% Mn), but the value of M does not change with the change of composition of Mn. Instead of changing its period with the change of the electron-atom ratio as observed in the long-period structures of noble-metal alloys, this alloy tends to distort tetragonally in order to keep the Brillouin-zone boundaries at the Fermi surface. This condition, however, requires a large distortion of the crystal and this distortion was found to be maintained by a preferential distribution of Mn atoms in a particular sublattice. This is the reason why such a long-period structure can exist over a wide composition range without changing its period. The preferential distribution of Mn atoms in the antiphase structure was also found to change the Cu₃Au-type ordered structure at low Mn content continuously to the CuAu-type ordered structure without the formation of a two-phase region. Such a continuous change between two superlattice phases has never been reported in other alloy systems.

The relative stability of Pd₃Mn II with respect to the other superlattices, along with the large tetragonal distortion, led us to conclude that the origin of the stability of the long-period superlattice in Pd-Mn alloys is the same as that found in the noble-metal alloys in the sense that these alloys tend to keep their Brillouin-zone boundaries at the Fermi surface. Based on the theory developed for the long-period superlattices of noble-metal alloys, the number of conduction electrons of the transition elements in the alloys can be estimated to be 3 for Mn and 0.6 for Pd. The similar

behavior of Al, Cu, or Mn when added to Pd₃Mn II also supports the present conclusion.

The general agreement of the experimental results, including those for the noble-metal alloys previously published, with the theory indicate that the type of argument adopted for the stabilization of the long-period structure, which is essentially an approximation valid for a long period, can also be applied without alteration to alloys with a short period, $M=2$. Indeed, there seems to be no fundamental difference between the two groups of alloys with $M=2$, i.e., those which change their period shorter than $M=2$ with a change in e/a , and those which do not, and the apparent difference can be ascribed to the magnitude of the "antiphase boundary energy." Among the latter, Pd-Mn alloys are peculiar in that they exist over a wide concentration range with a large tetragonal distortion caused by the preferential distribution of Mn atoms, whereas in Au₃Zn(H), Au₃Cd, etc. the increase in the distortion energy is so large that a change in structure occurs with a small change in the composition and thus limits the range of stability of these alloys.

Combining the results on normal long-period superlattices, it can be said that the electronic structure of alloys with long-period structures is understood fairly well. One important feature is the existence of the energy minimum at the point where the Brillouin-zone boundary touches the Fermi surface, when the electron energy of a system with a fixed number of electrons is plotted against the location of the Brillouin-zone boundary.¹⁵ This is shown clearly from the change of the period or from the distortion of long-period superlattices upon the change of the size of the Fermi surface. Theoretical arguments on whether such an energy minimum really exists or not in a three-dimensional crystal have been controversial. Moreover, the qualitative agreement of the tetragonal distortion of Pd₃Mn II with the theoretical curve indicates that the number of conduction electrons in such a transition-metal alloy is kept more or less constant for a relatively wide composition range. The results also give rather a clear image of how a large deviation from cubic symmetry can occur in a basically cubic crystal.

ACKNOWLEDGMENTS

Enlightening discussions with Dr. G. Honjo and Dr. A. Arrott of this Laboratory are greatly appreciated.

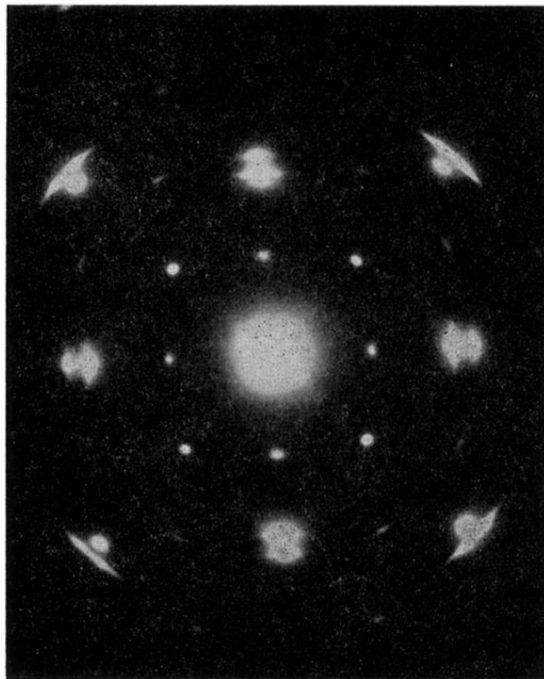


FIG. 10. Electron-diffraction pattern of a Pd-Mn alloy at around 34% Mn having the CuAu I structure.

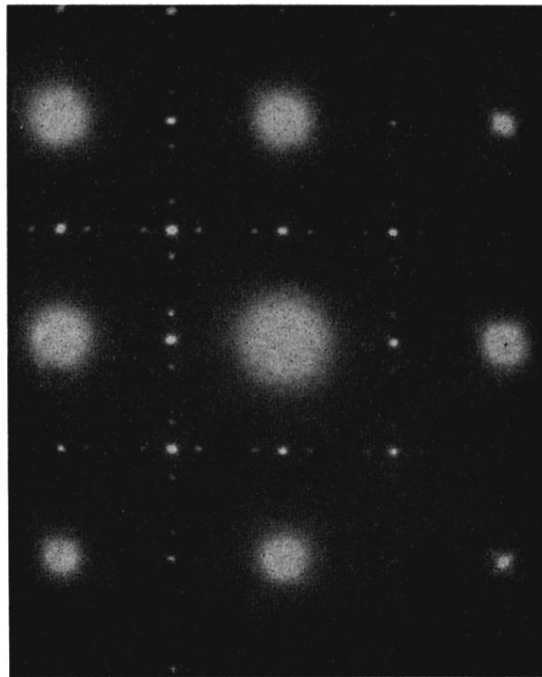


FIG. 3. Electron-diffraction pattern of an alloy having the $\text{Pd}_3\text{Mn II}$ structure, showing the characteristic splitting of the superlattice spots.

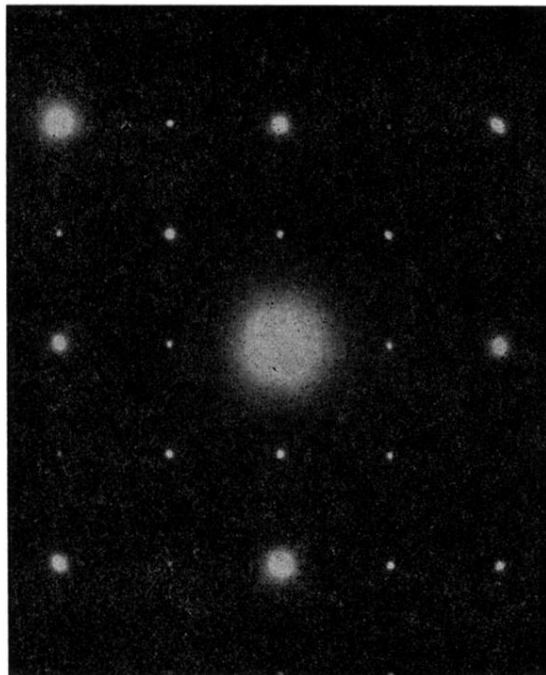


FIG. 4. Electron-diffraction pattern of a Pd-Mn alloy containing 20 at.%Mn which has the Cu_2Au -type ordered structure.

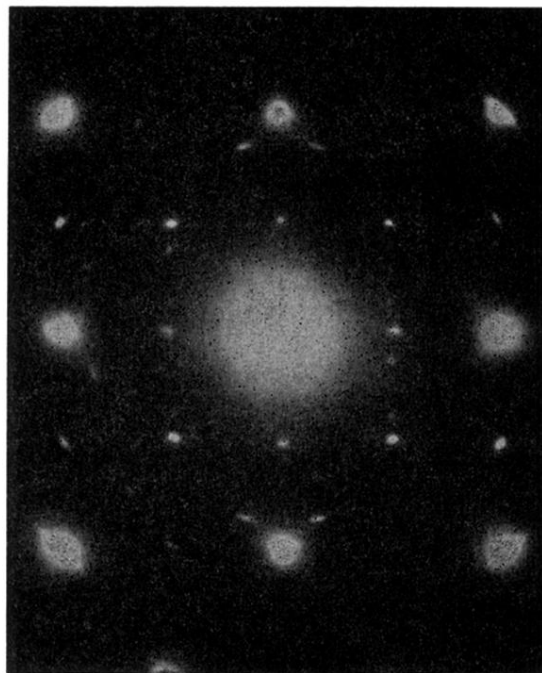


FIG. 6. Electron-diffraction pattern of an alloy having the Pd₂Mn II structure with a distortion $c/a \sim 0.95$.